Indian Journal of Pure & Applied Physics
Vol. 62, June 2024, pp. 451-463
DOI: 10.56042/ijpap.v62i6.8158

# New All-Optical Implementation of Fredkin Gate Suitable for Compact and Ultrafast Reversible Computing Applications

Mayank Srivastava[a*], Ajay Kumar[a], Kapil Bhardwaj[a], Devesh Kumar Srivastava[b], Ramendra Singh[c] & Dinesh Prasad[d]

[a]Department of Electronics and Communication Engineering National Institute of Technology, Jamshedpur Jharkhand 831 014, India

[b]SIT, Manipal University Jaipur, Jaipur, Rajasthan 303 007, India

[c]Department of Computer Science (IoT), RKGIT, Ghaziabad, Uttar Pradesh 201 003, India

[d]Department of Electronics and Communication Engineering, Jamia Millia Islamia, New Delhi 110 025, India

*Received 18 January 2024; accepted 27 February 2024*

This paper aims to propose a new all-optical implementation of Fredkin gate using micro-ring resonator (MRR) based logical switches. The proposed all-optical Fredkin gate scheme employs only five MRRs connected in a parallel branch topology, therefore found very compact and ultrafast as compared to many previously reported designs. The presented gate enjoys all-optical operation with no requirement for an additional wavelength converter. A detailed discussion of the all-optical switching mechanism of MRR has been presented and the logical behavior of the presented Fredkin gate has been demonstrated by using MATLAB simulations.

**Keywords:** MRR; All-optical design; Optical pumping; Fredkin gate

## 1 Introduction

Reversible logic, pioneered by Rolf Landauer in 1961[1], emerged to tackle the escalating energy consumption in computational processes. Traditional irreversible logic operations dissipate energy as heat at each computation step, exacerbated by information loss at the output. According to Landauer's principle, a logic system releases kT log 2 joules of heat energy for every lost bit of information, where 'k' is Boltzmann's constant, and 'T' is the system's absolute temperature. In high-speed communication networks, like internet-based systems, the substantial data volume necessitates numerous logic processors, resulting in significant information loss and subsequent heat generation.

Reversible computation, thriving in ideal physical conditions with almost zero power dissipation, proves pivotal. Reversible logic circuits exhibit a one-to-one mapping between input and output vectors, finding applications in nanotechnology, DNA computing, and quantum computing. Various reversible logic gates, including the Feynman gate, Fredkin gate, Toffile gate, and TR gate, have been developed. Notably, the Fredkin gate[2], invented by Ed Fredkin, serves as a universal logic gate, enabling both logical and arithmetic operations.

Optical implementation of logic operations has witnessed a surge in the last decade, capitalizing on optical systems' superior speed, security, and reliability over electrical counterparts. Optical switching, a critical component, is classified into two categories: electro-opto switching, where an external electrical signal controls optical signal switching, and all-optical switching, where both the signal and control signals are optical. All-optical switching, which is inherently more reliable, has garnered substantial attention from researchers.

The implementation of reversible logic and optical computing presents a promising avenue for addressing energy efficiency and computational speed simultaneously. This fusion not only mitigates heat dissipation issues associated with traditional computing but also harnesses the benefits of optical systems. The implementation of logical functions in the optical domain thrives on the efficient switching of optical signals in optical devices. Researchers have extensively explored this domain, reporting diverse logical circuits utilizing different optical components[3–45]. As technology continues to advance, the synergy between reversible logic and optical computing holds significant potential for shaping the future landscape of energy-efficient and high-speed computational systems.

*Corresponding author: (E-mail: mayank2780@gmail.com)

**State of Art: Reversible Logic Gates Implementation in Optical Domain**

In addition to the optical implementations of conventional irreversible logic functions/gates, various optical realizations of reversible logic functions like the Toffoli gate, Feynman gate, and Fredkin gate have also been presented in the literature[26-45]. The Fredkin gate implementations in the optical domain using various optical components have been reported in[32-35,39,41-45]. A tabular review of these previously reported Fredkin gate configurations has been presented in Table 1.

By careful investigation of Table 1, it can be seen that all-optical Fredkin and Feynman gates employing SOA have been presented in[32]. The Fredkin gate proposed in this paper employs two SOANOLMs and two optical couplers. Each SOANOLM is constructed by using three Gaussian optical pulse generators, three optical attenuators, two Gaussian optical filters, two ideal multiplexers, two traveling wave SOAs, couplers, power splitters, and power combiners. So, this Fredkin gate implementation requires excessive hardware and cannot be considered a compact and high-speed circuit. In[33]Fredkin gate employing two PSWs (based on SOA) and frequency-based beam routing by two optical multiplexers and a single de-multiplexer has been presented. The PSW comprises two polarization controllers, one tensile strained SOA, one polarization beam splitter (PBS), and an attenuator. The working of this system is very complicated as it is based on polarization switching of SOA. Implementation of an all-optical Fredkin gate employing SOA-based non-linear loop mirror has been developed in[34]. This gate is based on the terahertz optical asymmetric de-multiplexer that comprises a nonlinear loop mirror with an SOA. An All-optical realization of a modified Fredkin gate employing MZI-SOA has been developed in[35]and employs two SOAs, two polarization beam splitters, and two 3-dB couplers. The SOA or MZI-SOA-based reversible logic gates offer all-optical behavior but the performance of such constructed circuit is limited due to the low gain and phase response time of SOA. The MRR is also used for the all-optical implementation of reversible logic circuits. An all-optical reversible network design using micro-ring resonators has been

Table 1 — Previously reported Fredkin gates in the Optical Domain

| Ref. | Optical components used | Operation | Speed of operation | Switching mechanism |
|---|---|---|---|---|
| [32] | Gaussian optical pulse generators, couplers, optical attenuators, Gaussian optical filters, power splitters, ideal multiplexers, traveling wave SOAs, delay lines, and power combiners.(53) | All-optical | Low speed (Signal transmission through more than two cascaded optical components) | Power switching |
| [33] | Polarization controllers, tensile strained SOAs, polarization beam splitter, attenuator, optical multiplexers, and demultiplexers (11) | All-optical | Low speed (Signal transmission through more than two cascaded optical components) | Polarization based switching |
| [34] | polarization controllers, circulators,wavelength division multiplexers, 50:50 coupler, and SOA (9) | All-optical | Low speed (Signal transmission through more than two cascaded optical components) | Polarization based switching |
| [35] | MZI, two SOAs, polarization beam splitters, 3-Db beam splitter (8) | All-optical | Low speed (Signal transmission through more than two cascaded optical components) | Polarization based switching |
| [39] | Wide-band resonators, sharp resonators, and nonlinear ring resonators. (20) | All-optical | Low speed (Signal transmission through more than two cascaded optical components) | Power switching |
| [41] | Kerr switches and 50:50 couplers (8) | All-optical | Low speed (Signal transmission through more than two cascaded optical components) | Power switching |
| [42] | MZIs, nonlinearKerr elements,and phase shifters (22) | All-optical | Low speed (Signal transmission through more than two cascaded optical components) | Power switching |
| [43] | MZIs, splitters, (7) | Electro-optical | Low speed (Signal transmission through more than two cascaded optical components) | Power switching |
| [44] | Mach-Zehnder interferometers and multimode interference couplers (10) | non-all optical | Low speed (Signal transmission through more than two cascaded optical components) | Power switching |
| [45] | Heavily doped GeO2 fiber, polarization controllers, filters, circulators, couplers | All-optical | Low speed (Signal transmission through more than two cascaded optical components) | Polarization based switching |

reported in[36]. In[37] all-optical reversible Peres and Feynman-double logic gates employing silicon mirroring resonators have been reported. The MRR-based all-optical reversible TR gate and its applications in information processing have been discussed in[38]. In[39], an all-optical Fredkin gate was proposed which employs four wide-band resonators, twelve sharp resonators, and four nonlinear ring resonators. One another complicated Fredkin gate based on polarization switching of SOA has been reported in[40]. In[41] the switching of light from Kerr-type material has been used for designing the Fredkin gate. A total of six Kerr switches have been used in this configuration. So, on careful investigation of reported optical Fredkin Gate configurations it can be said that previously proposed optical Fredkin gates suffer one or more following disadvantageous features.

**(i)** Employment of a large number of optical components which requires more area on a chip

**(ii)** Cascaded architecture with multiple serial stages, which limit the speed of operation

**(iii)** Complex structure with the use of multiple splitters, combiners, phase shifters, etc. which makes operation very complex

**(iv)** Non all-optical operation

Therefore, the objective of this paper is to propose a new all-optical realization of Fredkin gate which enjoys the following advantageous features (i) a very compact structure with employment of only five MRRs (ii) The MRRs are connected in a parallel branch topology where in each branch, maximum two cascaded MRRs are placed so, maximum transmission delay is equals to only twice the switching time of single MRR. Therefore, an ultrafast operation is possible (iii) No requirement for wavelength conversion during operation and (iv) no requirement of splitters, combiners, phase shifters, *etc*.

Therefore, the proposed design achieves exceptional compactness and speed, outperforming previous implementations.

## 2 Concept of All-Optical Switching in MRR

The all-optical switching phenomenon can be considered as one of the most interesting concepts in advanced optical engineering. Several optical components enjoy the facility of all-optical switching and MRR is one of them. The MRR is a well-known optical system which found many applications in various optical signal processing operations but in the last decade, the MRR has attracted special attention due to its all-optical switching capability. This optical switching facility of MRR makes this component a suitable all-optical switch that can be used for all-optical implementation of digital logic. The structure of MRR is shown in Fig. 1.

It is clearly illustrated in Fig. 1 that the MRR structure includes a ring resonator and two linear waveguides. The working concept of MRR structure is founded on the optical coupling between the resonator ring and waveguides. The extent of coupling between the input waveguide and the ring resonator is described by coupling coefficient "$k_1$" while "$k_2$" is defined as the coupling coefficient between the ring resonator and output waveguide. The "$k_1$" basically describes the fraction of input power (power of input signal applied at input port) transmitted to the resonator ring. In the same manner, the "$k_2$" can be described as the fraction of power transmitted from the ring resonator to the drop port of the output waveguide. The power available in the ring (which is transferred to the ring resonator from the input port) travels alongside the periphery of the ring resonator. If the periphery of the ring is equaled to the integral multiple of the wavelength of the applied input signal then after one rotation of the signal in the ring, the constructive interference takes place, and maximum power is found available at the drop port in the form of periodic fringes. This event is called "On Resonance". In this state, the signal power at the through port is found minimal. So, this complete process can be viewed as the switching of the optical signal from the input port of the input waveguide to the drop port of the output waveguide. It is important to mention here that in a condition of destructive interference, the signal power found available at the drop port is minimal. In this state, the power at the

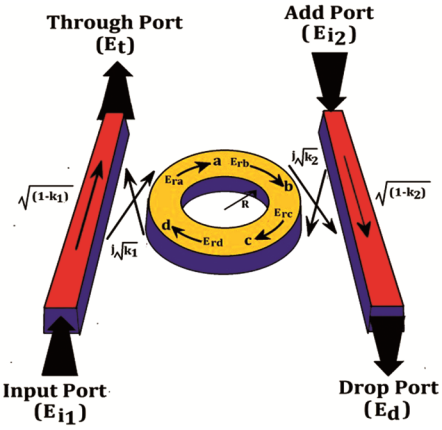


Fig. 1 — Layout of Micro-ring resonator structure

through port is found maximum. The process of all-optical switching and its mathematical analysis has been discussed in[14].

## 3 Idea of Fredkin Gate

The Fredkin gate is one of the most popular reversible logic gates which can be considered as a universal gate as any arithmetic or logical function can be implemented by using Fredkin gate(s) only. It is a three-input/three-output gate that transmits the first bit as it is and swaps the last two bits if and only if the first bit is "1". Based on this definition, the two possible behavioral representations of

### Proposed MRR-based all-optical Fredkin Gate

Fredkin gate using irreversible logic operands can be shown in Fig. 2. The implementation of the Fredkin gate logic idea illustrated in Fig. 2 using an irreversible binary two-input logic gate has been shown in Fig. 3.

The truth table of Fredkin Gate is described in Table 2. It is important to note here that numbers of 1s and 0s are the same in each input-output combination which indicates the no-loss of bit(s) and zero power dissipation.

The logical design of the Fredkin gate shown in Fig. 4 employs four 2-input AND gates, two 2-input OR gates, and one NOT gate.

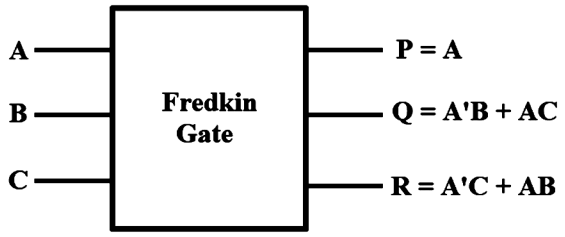


Fig. 2 — Symbolic representations of Fredkin gate

Now, these two designs can be converted into MRR-based all-optical configurations simply by using the previously reported MRR-based AND, OR, NOT, and XOR logic gates configurations. It is well understood that due to its switching capability a single MRR structure can simulate the behavior of a NOT gate in the all-optical domain. The MRR-based all-optical realization of two-input AND gate has been presented in[15] which employs only two MRRs. The two-input OR gate implementation in an all-optical domain employing six MRRs has been reported in[19] and a two-input XOR gate implementation using two MRRs has been discussed in[20]. Therefore by using these all-optical logic gates configurations, the logic design shown in Fig. 3 can be converted into an all-optical Fredkin gate based on MRRs. Such constructed all-optical Fredkin gate realization based on the scheme shown in Fig. 4 requires seventeen MRRs. Also, the implementations require wavelength converters. Due to such excessive requirement of optical components, these optical circuits require a large area of integration, and also speed is limited due to a large number of stages of operation. Therefore, in this work, we have proposed a new improved all-optical realization of Fredkin gates using MRRs. The proposed scheme is very compact and ultra-fast with the employment of only five MRRs. This scheme is

Table 2 — Truth table of Fredkin Gate

| Inputs | | | Outputs | | |
|---|---|---|---|---|---|
| A | B | C | P | Q | R |
| 0 | 0 | 0 | 0 | 0 | 0 |
| 0 | 0 | 1 | 0 | 0 | 1 |
| 0 | 1 | 0 | 0 | 1 | 0 |
| 0 | 1 | 1 | 0 | 1 | 1 |
| 1 | 0 | 0 | 1 | 0 | 0 |
| 1 | 0 | 1 | 1 | 1 | 0 |
| 1 | 1 | 0 | 1 | 0 | 1 |
| 1 | 1 | 1 | 1 | 1 | 1 |

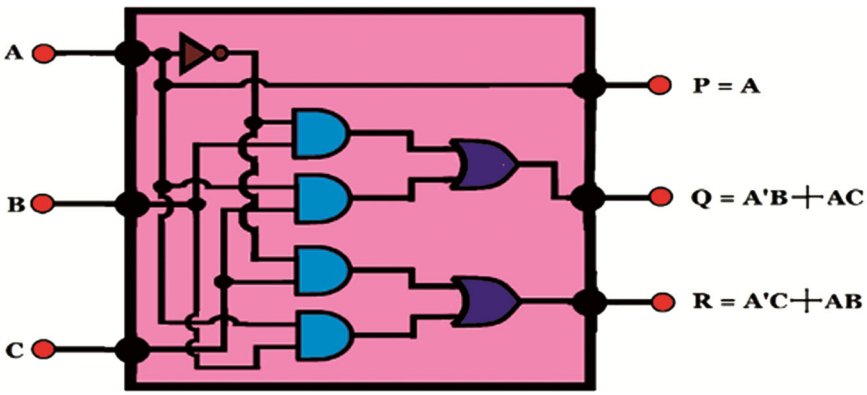


Fig. 3 — Fredkin gate implementation using irreversible binary logic gates: using NOT, ANDs, and ORs logic gates

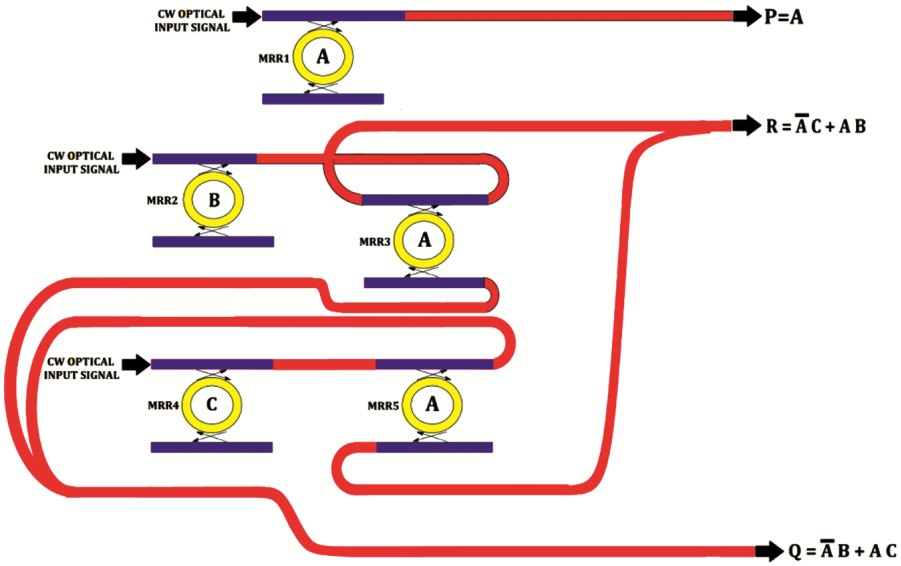


Fig. 4 — Proposed five MRRs based on all-optical realization of Fredkin gate

based on the behavioral model of Fredkin gate shown in Fig. 2. The presented all-optical schemes of Fredkin gate do not require any wavelength converter(s).

The proposed MRR based all-optical realization of Fredkin gate has been shown in Fig. 4, which employs only five MRR structures.

As the developed design is a parallel topology so, the transmission delay of this gate is also very low which is equal to twice the switching period of an MRR as the switching through only two MRRs is required to produce output Q or R (while to generate the output P the switching through only one MRR is required). Therefore, this implementation can be considered as the highly compact and ultra-fast all-optical realization of the Fredkin gate. The working of this gate can be described as;

**Case 1: When A=1, B=0, C=0**

when A=1, the input signal at the input port of MRR1 gets switched to the through port of MRR1 due to the high status of the pump signal, and high transmission is found available at output P. So, P is at logic high status. The optical signal applied on the input port of MRR2 gets transferred to the drop port of MRR2 as the status of the control signal at MRR2 is low. In the same manner, the input optical signal applied at the input port of MRR4 is transferred to the drop port of the same MRR due to the low status of control signal C. Therefore, the low or no signal appears at both the outputs Q and R and the status of both of these outputs can be considered as logic low.

**Case 2: When A=1, B=1, C=0**

Due to the high status of A, the output P is found at logic high status same as the previous case. The optical signal applied on the input port of MRR2 gets transferred to the through port of MRR2 due to the high pump applied on MRR2. This signal reaches the through port of MRR3 due to the high-status control applied on MRR3. Thus the output R is found as logic High. Due to C=0, the input signal applied at the input port of MRR 4 gets switched to the drop port of MRR4, Hence low transmission is found at output Q. This shows the logic low status of Q.

**Case 3: When A=1, B=0, C=1**

Again in this case also due to A=1, the output P is found at a logic high status. The optical signal applied on the input port of MRR2 gets transferred to the drop port of MRR2 as the status of the pump signal is low. This shows the low signal transmission at port R and the status of R is logic low. Due to C=1 and A=1, the input optical signal applied at the input port of MRR4 gets transferred to port Q. This high transmission at Q can be considered as logic high.

**Case 4: When A=1, B=1, C=1**

Similarly like the previous three cases, due to the high status of A, the output P is found at logic high status. The input signal applied at the input port of MRR2 was found available at port R as control signals for MRR2 and MRR3 are high-status signals. So, the status of R is logically high. Similarly, the high transmission is achieved at output port Q due to

high pump signals applied on MRR4 and MRR5 and Q is also found at logic high status.

**Case 5: When A=0, B=0, C=0**

Due to A=0, the input signal at the input port of MRR1 gets switched to the drop port of MRR1 and no/low transmission is found available at output P, and the status of P can be said logic low. The optical signal applied on the input port of MRR2 gets transferred to the drop port of MRR2 as the status of the control signal at MRR2 is low. In the same manner, the input optical signal applied at the input port of MRR4 is transferred to the drop port of the same MRR due to the low status of control signal C. Therefore, the low or no signal appears at both the outputs Q and R and the status of both of these outputs is logic low.

**Case 6: When A=0, B=1, C=0**

Due to the low status of A, the output P is found at logic low status same as the previous case. The optical signal applied on the input port of MRR2 gets transferred to the through port of MRR2 (due to high pump signal) and this signal reaches the drop port of MRR3 as the control signal applied on MRR3 is high. So, the status of Q is found logic high. Due to C=0, the input signal applied at the input port of MRR 4 gets switched to the drop port of MRR4. In this case, the status of output R is logic low.

**Case 7: When A=0, B=0, C=1**

Again due to the low status of A, the logic low status is found available at output P. Due to the low pump, the optical signal applied on the input port of MRR2 gets transferred to the drop port of MRR2. As, C=1 and A=0, the input optical signal applied at the input port of MRR4, gets transferred to the port Rand shows the logic high status of R. In this situation, no Q is found at logic low as no signal reaches it.

**Case 8: When A=0, B=1, C=1**

Similarly like the previous three cases, due to the low status of A, the output P is found at logic low status. The input signal to MRR2 found available at port Q as control signals for MRR2 is high while the pump signal to MRR3 is low. The input signal to MRR4 gets transferred to the drop port of MRR5 due to the high pump signal on MRR5 and a low control signal on MRR4. Hence the status of R is logic high.

***Mathematical Model of Presented MRR-based All-optical Fredkin Gate***

By using the mathematical model of MRR presented in[15], the mathematical model of proposed Fredkin gate shown in Fig. 4 has been developed.

The output P is fetched from through the port of MRR. The transfer function for port P can be evaluated as;

$$\frac{E_P}{E_i} = \frac{D\sqrt{1-k_1} - D\sqrt{1-k_2}x^2exp^2(j\phi)}{1-\sqrt{1-k_1}\sqrt{1-k_2}x^2exp^2(j\phi)} \quad \ldots (1)$$

The output R is fetched as the combination of signal from the through port of MRR3 and drop port of MRR 5. Therefore, the transfer function for output R can be found as;

$$\frac{E_R}{E_i} = \left(\frac{D\sqrt{1-k_1} - D\sqrt{1-k_2}x^2exp^2(j\phi)}{1-\sqrt{1-k_1}\sqrt{1-k_2}x^2exp^2(j\phi)}\right)^2 + \left\{\left(\frac{D\sqrt{1-k_1} - D\sqrt{1-k_2}x^2exp^2(j\phi)}{1-\sqrt{1-k_1}\sqrt{1-k_2}x^2exp^2(j\phi)}\right) \times \left(\frac{-D\sqrt{k_1k_2}x\exp(j\phi)}{1-\sqrt{1-k_1}\sqrt{1-k_2}x^2\exp^2(j\phi)}\right)\right\} \quad \ldots (2)$$

Similarly, the output Q is fetched as the combination of signal from the through port of MRR5 and drop port of MRR 3. Therefore, the transfer function for output Q can be found as;

$$\frac{E_Q}{E_i} = \left(\frac{D\sqrt{1-k_1} - D\sqrt{1-k_2}x^2exp^2(j\phi)}{1-\sqrt{1-k_1}\sqrt{1-k_2}x^2exp^2(j\phi)}\right)^2 + \left\{\left(\frac{D\sqrt{1-k_1} - D\sqrt{1-k_2}x^2exp^2(j\phi)}{1-\sqrt{1-k_1}\sqrt{1-k_2}x^2exp^2(j\phi)}\right) \times \left(\frac{-D\sqrt{k_1k_2}x\exp(j\phi)}{1-\sqrt{1-k_1}\sqrt{1-k_2}x^2\exp^2(j\phi)}\right)\right\} \quad \ldots (3)$$

## 4 Simulation Results using MATLAB

The all-optical switching operation in MRR can be understood by MATLAB numerical simulation as discussed in[14].In the MRR structure, the coupling coefficient ($k_1$ & $k_2$) are the most important parameters for deciding the ideal switching mechanism. The switching in MRR is based on the mechanism that, in the absence of the control pump signal, an optical signal can be observed at the drop port, whereas with the application of the control signal, the optical signal is found available at the through port. For getting optimum switching, the most optimized value of the coupling coefficient ($k_1$ & $k_2$) needs to be calculated.The switching operation in MRR is also dependent upon the radius of the ring resonator as the constructive or destructive interference inside the ring solely depends upon the periphery of the ring. From[14], it has been found that

for $k_1 = k_2$= 0.25, and radius value of 7.089 µm, the MRR offers excellent switching behaviour. As shown in Fig. 5 (taken from[14]), in MRR, switching of an optical signal from the input port to the through port or from the input port to the drop port takes place depending upon the level of the optical control signal applied on the top of the ring resonator. In Fig. 5, the first row describes the control signal status. The second row denotes the status of the through port while the third row represents the response at the drop port corresponding to the applied control signal. The control signal wavelength is 1550 nm. The Fig. 6 shows the 3D simulation of the MRR structure demonstrating the distribution of the normalized optical intensity pulse with the absence and presence of the pump signal.

3D simulation of the MRR structure as a switch, representing the distribution of normalized optical intensity pulse with the (a) Absence, (b) Presence of pump signal

The various performance parameters of the employed MRR switch[14], have been evaluated by MATLAB simulations and mentioned in Table 3.

The values of parameters such as FSR, FWHM, Quality factor, on-off ratio and Fitness factor as mentioned in Table 3 have been evaluated from the simulation results illustrated in Fig. 7. Moreover the variations of Extinction ratio and Contrast ratio with respect to design parameters (coupling coefficients and radius of MRR ring) have been shown in Figs 8 & 9 respectively. The switching rise time and switching fall time of MRR switch have been determined by switching time response plot shown in Fig. 10.

The effective refractive index of the ring structure can be represented as

$$n_{eff} = n_0 + n_2 . I = n_0 + \frac{n_2}{A_{eff}} P.$$

Where, $n_0$ and $n_2$ are the linear and non-linear refractive index, respectively and I and P are the intensity and power of the optical pump signals.

Table 3 — Performance parameters of employed MRR switch

| Switching Parameter | Values |
|---|---|
| Free spectrum range (FSR) | 43nm |
| Full width with half minimum (FWHM) | 2nm |
| Quality factor | 750 |
| On off ratio | 41.049 dB |
| Fitness factor | 21.5 |
| Extinction ratio | 18.98 dB |
| Contrast ratio | 19.54 dB |
| Switching rise time | 2.531 ps |
| Switching fall time | 2.52 ps |

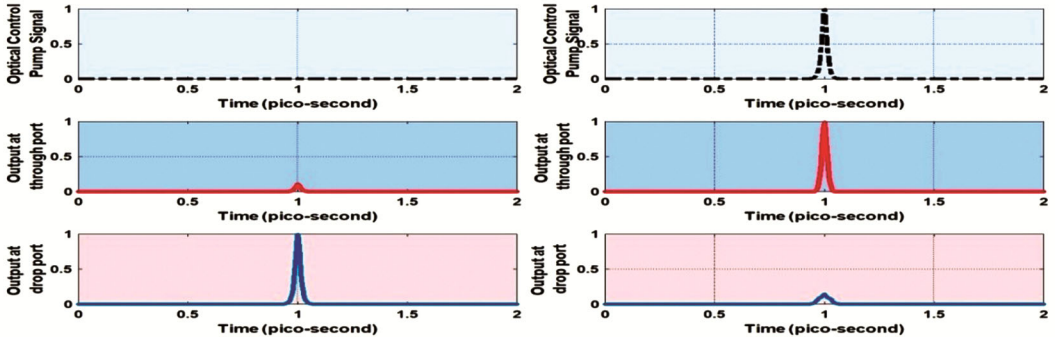


Fig. 5 — Demonstration of optical-switching in the MRR[14]

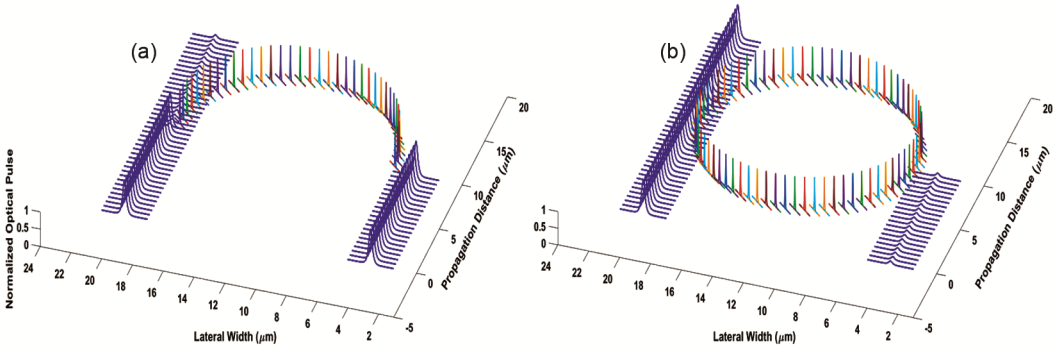


Fig. 6 — 3D simulation of the MRR structure as a switch, representing the distribution of normalized optical intensity pulse with the (a) Absence, (b) Presence of pump signal

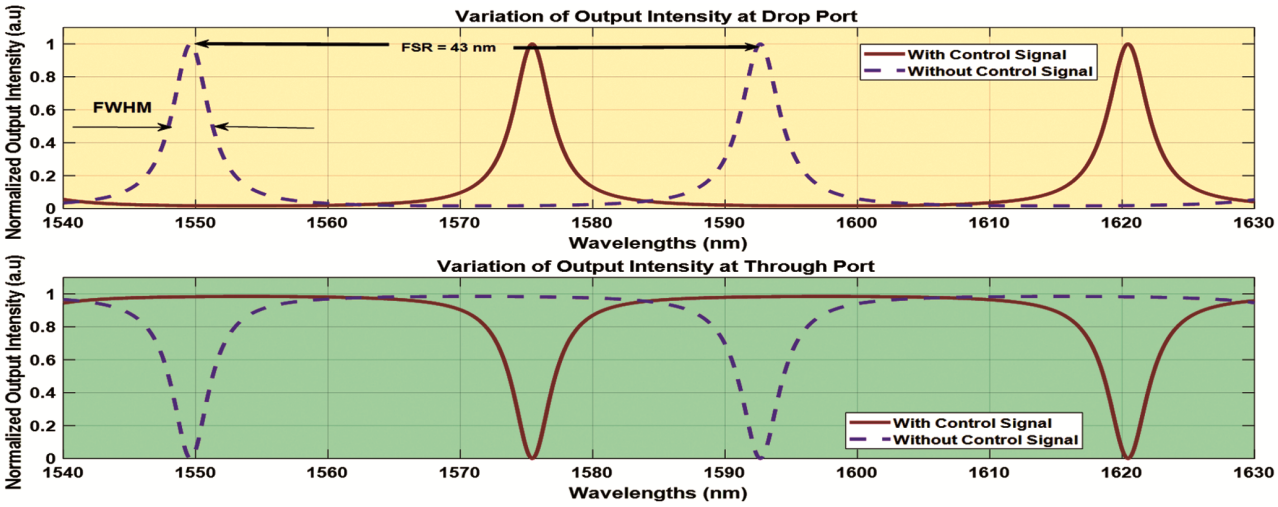


Fig. 7 — Fluctuation in intensity at the through port and drop port under different conditions[14]

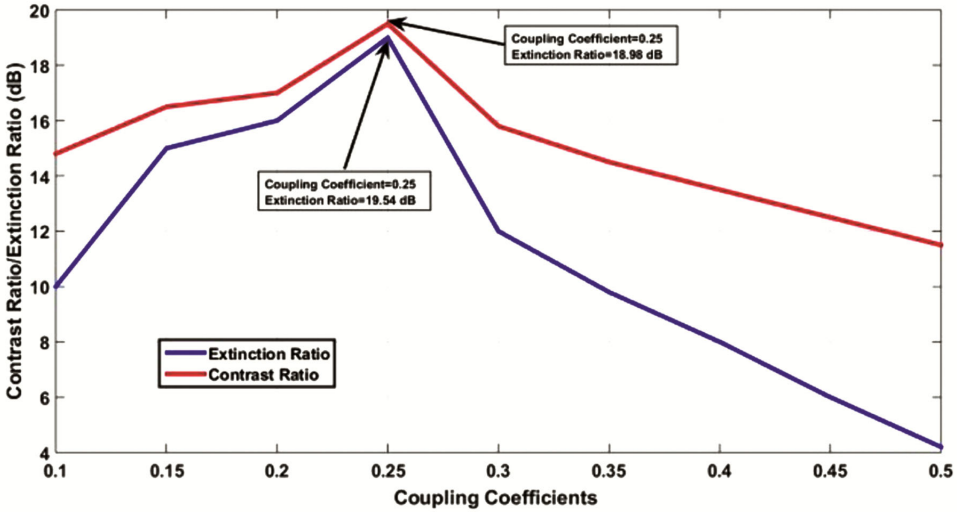


Fig. 8 — Variation of contrast ratio and extinction ratio w.r.t coupling coefficients

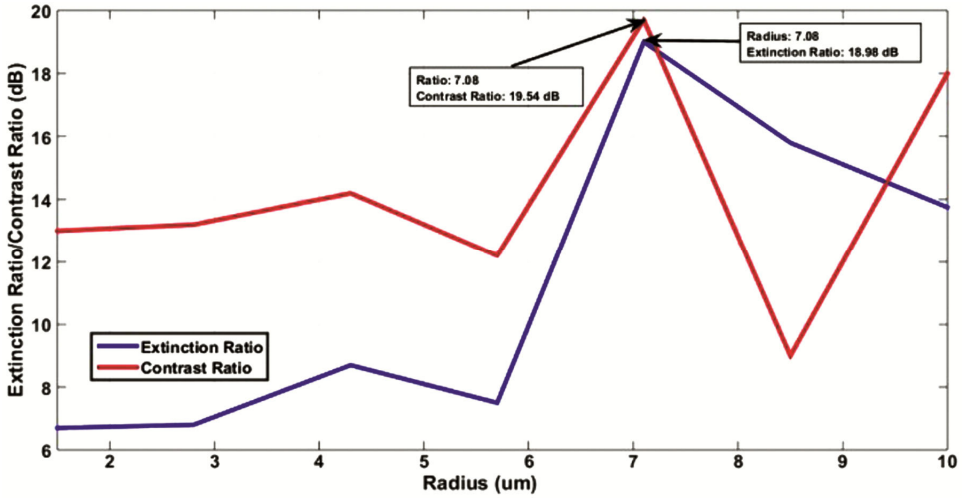


Fig. 9 — Variation of contrast ratio and extinction ratio w.r.t ring radius

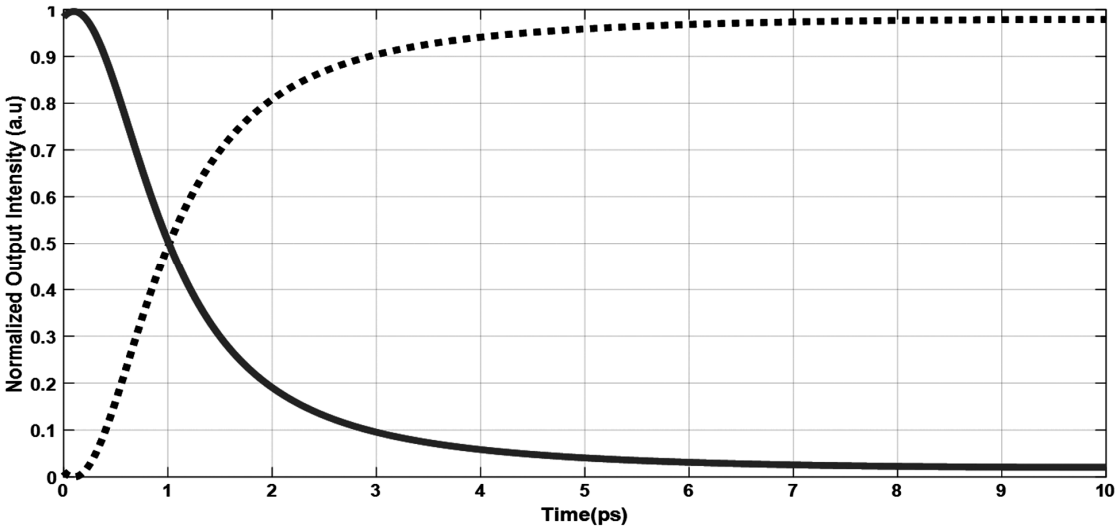


Fig. 10 — Switching Time response plot indicating Rise Time and Fall Time

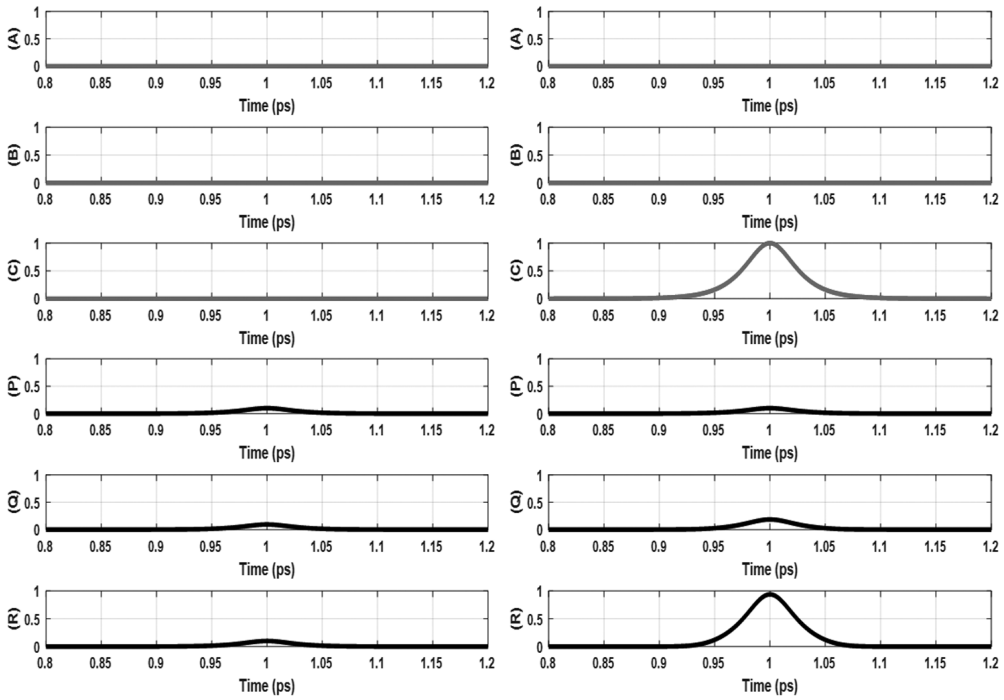


Fig 11 — MATLAB simulation result of the proposed Fredkin logic gate shown in Figure 5 for the input combinations ABC → 000 and ABC → 001

The value of the change in the effective index with the application of the control pump power is $3 \times 10^{-3}$, linear refractive index $n_0$ is 3.37, and the non-linear refractive index $n_2$ is $4 \times 10^{-18}\ cm^2/W$.

The value of pump power applied is 2.552 mW which is sufficient to induce a phase shift of π.

Now, to validate the workability of proposed MRR-based all-optical Fredkin gate implementations, the numerical simulations have been executed using the MATLAB simulation tool. For simulation purposes, the MRR parameters, described in Table 3, have been used.

The simulation results of the all-optical implementation of the Fredkin gate shown in Fig. 4 have been illustrated in Figs. 11-14. Fig. 11, shows the behavior of the presented Fredkin gate for input signals A = 0, B = 0, C = 0 and A = 0, B = 0, C = 1. The first column of Fig.11 shows the inputs A = 0,

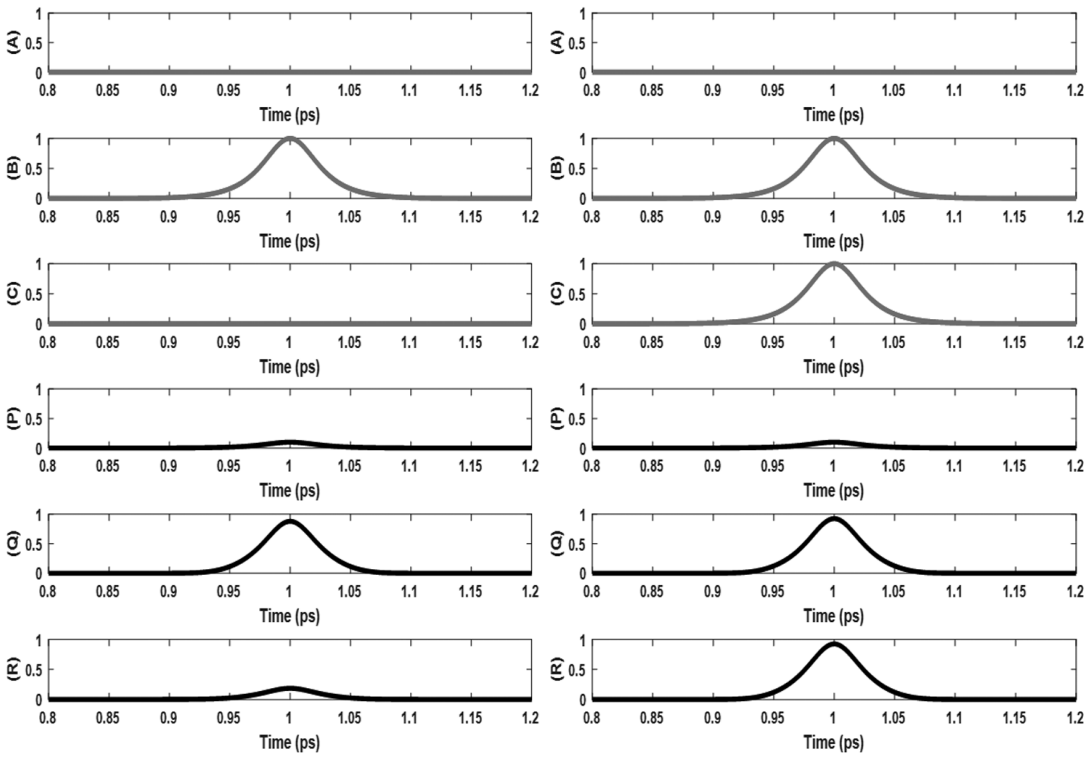


Fig. 12 — MATLAB simulation result of the proposed Fredkin logic gate shown in Figure 5 for the input combination ABC → 010 and ABC → 011

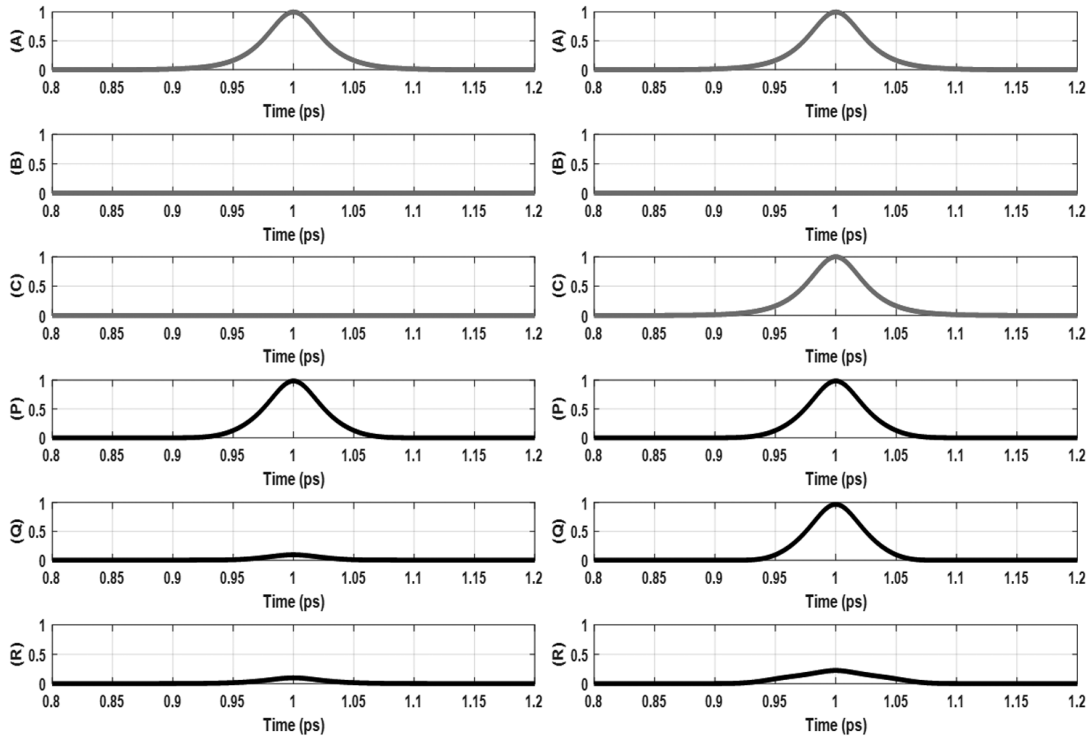


Fig. 13 — MATLAB simulation result of the proposed Fredkin logic gate shown in Figure 5 for the input combination ABC → 100 and ABC → 101

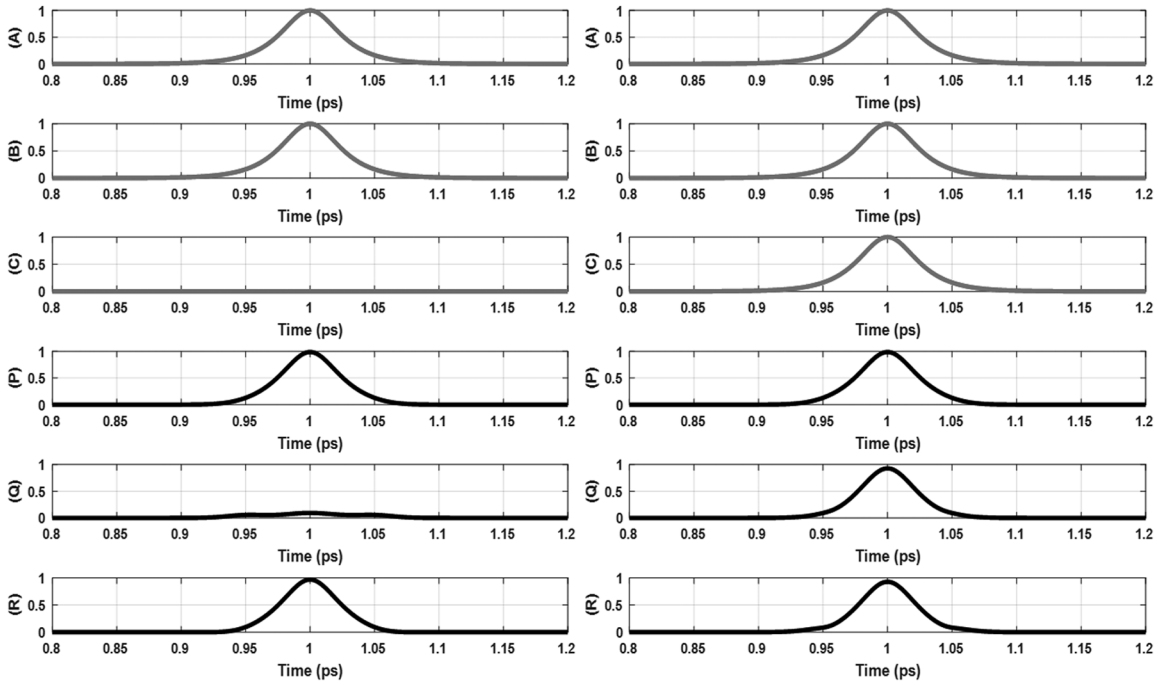


Fig. 14 — MATLAB simulation result of the proposed Fredkin logic gate shown in Figure. 5 for the input combination ABC → 110 and ABC → 111

B = 0, C = 0 and the status of outputs P Q, and R. It is clear here that for inputs A = 0, B = 0, C = 0, the status of outputs P, Q and R are 0, 0 and 0 respectively. Similarly, the second column of Fig. 10, shows the inputs and outputs for A = 0, B = 0, and C = 1. In the same manner, Figs. 12-14, show the behavior all-optical Fredkin gate shown in Fig. 4 for inputs (A = 0, B = 1, C = 0 and A = 0, B = 1, C = 1) and (A = 1, B = 0, C = 0 and A = 1, B = 0, C = 1), and (A = 1, B = 1, C = 0 and A = 1, B = 1, C = 1) respectively. On careful investigation of Fig. 11-14 it can be seen that the all-optical Fredkin gate shown in Fig. 4 verifies the Fredkin gate truth table described in Table 2. Therefore, it is confirmed that the developed all-optical design shown in Fig. 4 simulates the behavior of Fredkin gate.

To calculate the insertion losses experienced at different outputs of the proposed gate, MATLAB simulations have been performed to evaluate the insertion losses in a single MRR in different states. The simulation outcomes reveal that when no control pump signal is applied to the MRR ring, the insertion loss through the port is -32.9 dB, and at the drop post is -0.965 dB. In the presence of a pump signal, the insertion loss at the through port is found to be -2.65 dB and at the drop port, its value is -31.3 dB. The insertion losses at different outputs of the proposed Fredkin gate have been evaluated and given in Table 4.

Table 4 — Insertion loss found at various outputs of presented Fredkin Gate under different operating conditions

| Logic states of Inputs | | | Insertion loss at outputs | | |
|---|---|---|---|---|---|
| A | B | C | P | R | Q |
| 0 | 0 | 0 | -32.9 dB | -33.865 dB | -33.865 dB |
| 0 | 0 | 1 | -32.9 dB | -3.615dB | -33.865 dB |
| 0 | 1 | 0 | -32.9 dB | -32.9 dB | -3.615dB |
| 0 | 1 | 1 | -32.9 dB | -3.615dB | -3.615dB |
| 1 | 0 | 0 | -2.65 dB | -35.52 dB | -35.52 dB |
| 1 | 0 | 1 | -2.65 dB | -33.95 dB | -5.30 dB |
| 1 | 1 | 0 | -2.65 dB | -5.30 dB | -33.95 dB |
| 1 | 1 | 1 | -2.65 dB | -5.30 dB | -5.30 dB |

## 5 Experimental Realization Aspects

In this paper, a new all-optical configuration for simulating the behavior of reversible Fredkin gates employing MRRs has been reported. The proposed configuration is found

The proposed Fredkin gate is employed by using MRRs. So, in the experimental implementation of this gate, the most important thing is designing of desired MRR switch. So, while designing the MRRs for this structure following aspects need to be considered.

(i) The Selection of suitable material for MRR fabrication is very important as optical properties influence the performance of MRR significantly.

The fabrication technique of MRR is also decided on the basis of material used.

(ii) The physical designing of MRR structure is a very important aspect, which includes proper designing of MRR waveguides and Ring, proper coupling between ring and input/output waveguides, proper spacing between ring and waveguides *etc*.

(iii) The optical losses in MRR should be under permissible limit

(iv) The influence of temperature and good stability with respect to temperature is also a key aspect

(v) Compatibility of MRR with input signal sources

In the proposed Fredkin gate experimental implementation, the simultaneous application of the control pump signal is one of the most important aspects. However, the simultaneous applications of control pump signals, $e.g., A, B$ and $C$ signal can be applied using the approach of diffractive beam splitter techniques. The unit involves splitting the laser into multiple beams and simultaneously focusing on multiple points by combining lenses or focusing lenses. It can be used with multi-mode and single-mode lasers. It provides the facility of easy alignment, and in this technique, splitting characteristics remain independent of beam incidence position.

Figure 15 shows the basic arrangement of the diffractive beam splitter technique, which consists of a diffractive beam splitter and a focusing lens. Spot pitch is proportional to the focal length. The working principle can be represented using Fig. 16.

The collimated laser beam is allowed to pass through the beam splitter with the pre-specified separation angle. The well-focused spots can be achieved with a specific distance by adding a focusing lens after the diffractive beam splitter. The comparison of proposed MRR-based Fredkin gate with previously reported optical Fredkin gates has been given in Table 5.

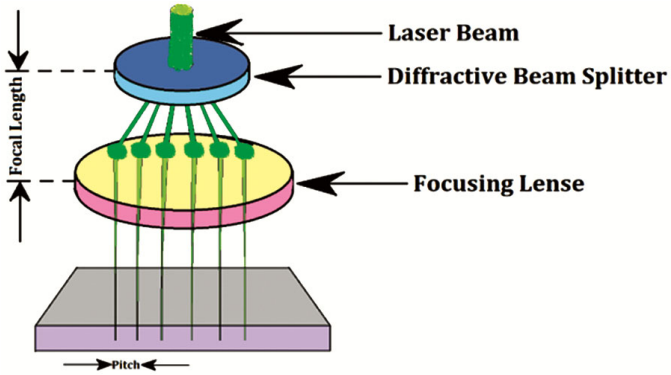


Fig. 15 — Diffractive Beam Splitter

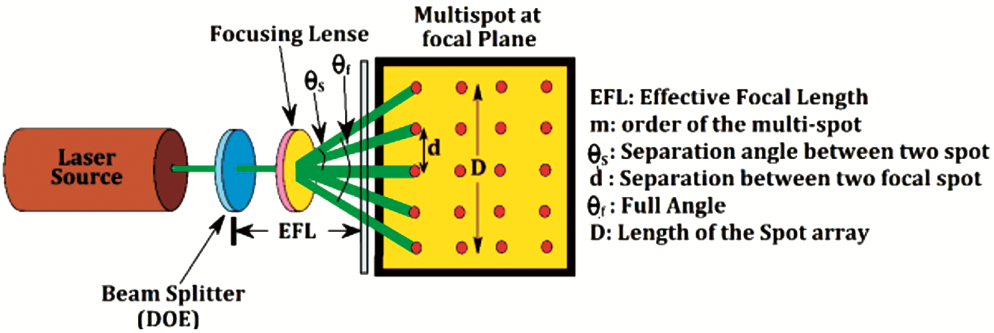


Fig. 16 — Schematic view of Set up of Diffractive Optical Element

Table 5 — Comparison of proposed MRR-based Fredkin gate with previously reported optical Fredkin gates

| Ref. | Input signal | control signal | Switching mechanism | Data rate | Biasing current | Delay |
|---|---|---|---|---|---|---|
| [32] | 1552nm | Optical (1545nm) | Power switching | 10Gb/s | 160-180mA | 130ps |
| [34] | 1552nm, 1554nm | Optical (1552nm) | Power switching | 1Gb/s | 100mA | 100ps |
| [35] | 1500nm | Optical (1500nm) | Power switching | 50Gb/s | 600mA | Not given |
| [43] | 1300nm | Electrical (6.75V) | Power switching | 100Gb/s | NA | Not given |
| Proposed | 1540nm | Optical (1550nm) | Power switching | 200Gb/s | NA | 5.062ps |

## 6 Conclusion

In this paper, a new all-optical configuration for simulating the behavior of reversible Fredkin gates employing MRRs has been reported. The proposed configuration is found very compact and employs only five MRRs. The presented design is a parallel topology and employs a maximum of two nos. of MRR in each parallel branch. Therefore, offers ultra-fast speed of operation. The MATLAB simulations have been performed to understand the switching mechanism of MRR and to achieve the optimum parameter values of the used MRR-based switch. The logical behavior of the presented all-optical realization of Fredkin gate has also been validated through MATLAB simulations.

## References


1 Hill M T, de Waardt H, Khoe G D, *IEEE J Quant Electron*, 37 (2001) 405.
2 Kabilan A P, Susan C X & Elizabeth C P, *Int Conf Comput Commun Network Technol*, (2010) 1.
3 Liu W, Yang D, Shen G, Tian H & Ji Y, *Opt Laser Technol*, 50 (2013) 55.
4 Jalila M A, Amirib I S, Teekac C, Alib J & Yupapinc P P, *Phys Exp*, 1 (2011) 15.
5 Thongmeea S & Yupapinb P P, *Int Sci Social Sci Eng Energy Conf Eng Sci Manag Pro Eng*, 8 (2011) 217.
6 Luangxaysana K, Phongsanam P, Mitatha S, Yoshida M, Komine N & Yupapin P P, *Inf Technol J*, 11 (2012) 1470.
7 Nadimi P, Caviglia D D & Di Z E, *World Acad Sci Eng Technol*, 71 (2012) 648.
8 Ma S, Chen Z, Sun H & Dutta N K, *Opt Exp*, 18 (2010) 6417.
9 Zoiros K E, Papadopoulos G, Houbavlis T, Kanellos G T, *Opt Commun*, 258 (2006) 114.
10 Karim M A, Awwal A A S & Cherri A K, *Appl Opt*, 26 (1987) 2720.
11 Raghuwanshi S K, Kumar A & Kumar S, *Opt Eng (SPIE)*, 52 (2013) 035002.
12 Gayen D K, Bhattachryya A, Chattopadhyay T & Roy J N, *J Lightwave Technol*, 30 (2012).
13 Houbavlis T, Zoiros K E, Kanellos G & Tsekrekos C, *Opt Commun*, 232 (2004) 179.
14 Kumar A, Kumar M, Jindal S K, Raghuwanshi S K & Choudhary R, *Opt Quant Electron*, 53 (2021) 31.
15 Kumar A, Kumar S & Raghuwanshi S K, *Optik*, 125 (2014) 5764.
16 Kumar A, Kumar S & Raghuwanshi S K, *Opt Commun*, 324 (2014) 93.
17 Kumar A & Raghuwanshi S K, *Opt Quant Electron*, 47 (2015) 2117.
18 Raghuwanshi S K, Kumar A & Chen N K, *Opt Commun*, 333 (2014).
19 Shekhar P, Kumar A, Ahmad A & Srivastava M, 2019 *IEEE Int Conf Elect, Electron Comput Eng (UPCON)*, (2019) 1.
20 Kumar A & Raghuwanshi S K, *Optik*, 127 (2016) 8751.
21 Li L & Sun J*, J Mod Opt*, 59 (2012) 809.
22 Zhang L, Ding J, Tin Y, Ji R, Yang L, Chen H, Zhou P, Lu Y, Zhu W & Min R, *Opt Express*, 20 (2012) 11605.
23 Kumar A, *Opt Quant Electron (Springer),* 48 (2016) 460.
24 Kumar A, *Opt Quant Electron (Springer)*, 48 (2016) 477.
25 Kumar A, *Opt Quant Electron (Springer))*, 51 (2019) 191.
26 Taraphdar C, Chattopadhyay T & Roy J N, *Opt Laser Technol*, 42 (2006) 249.
27 Bordoloi K, Theresal T & Prince S, *Int Conf Commun Signal Process*, (2014).
28 Kumar S, Chanderkanta & Raghuwanshi S K, *Appl Opt*, 55 (2016) 5693.
29 Rao D G S, Swarnakar S & Kumar S, *Appl Opt*, 59 (2020) 11003.
30 Katti R & Prince S, *Opt Quant Electron*, 48 (2016) 63.
31 Taraphdar C, Chattopadhyay T & Roy J N, *Opt Laser Technol*, 42 (2010) 249.
32 Ghazali N F, Wahid M H A, Ahmad H N A, Juhari N & Shahimin M M, *AIP Conf Proceedings*, 2045(1), 10.1063/1.5080892.
33 Mandal D, Mandal S & Garai S K, *Opt Laser Technol*, 72 (2015) 33.
34 Poustie A J & Blow K J, *Opt Commun*, 174 (2000) 317.
35 Chattopadhyay T, *IEEE J Select Top Quant Electron*, 18 (2012) 585.
36 Chattopadhyay T, *IEEE J Quant Electron*, 51 (2015) Article no. 6500108, doi: 10.1109/JQE.2015.2406667.
37 Sethi P & Roy S, Special Issue on Reversible Computing, *Springer Trans Comput Sci, XXIV, LNCS,* 8911 (2014) 21.
38 Roy J N & Rakshit J K, *12th Int Conf Fiber Opt Photon, IIT Kharagpur*, 2014.
39 Hassangholizadeh-Kashtiban M, Alipour-Banaei H, Tavakoli M B & Sabbaghi-Nadooshan R, *Appl Opt*, 59 (2020) 635.
40 Mandal D, Mandal S & Garai S K, *Opt Laser Technol*, 72 (2015) 33.
41 Dey S, De P & Mukhopadhyay S, *Optoelectron Lett*, 15 (2019) 317.
42 Cohen E, Dolev S & Rosenblit M, *Nature Commun*, 7, Art. no., 11424, (2016).
43 Kumar S, Chanderkanta & Raghuwanshi S K, *Appl Opt*, 55 (2016).
44 Yu R, Zhang J, Chen W, Wang P, Li Y, Li J, Fu Q, Dai T, Yu H & Yang J, *Appl Opt*, 228 (2021).
45 Kostinski N, Fok M P & Prucnal P R, *Opt Lett*, 34 (2009).